Journal of Testing and Evaluation, Sept 2004 Vol XX, No. X
Paper ID: 1234
Available online at: www.astm.org
Published XXXX

Michael J. Verrilli, James A. DiCarlo, HeeMann Yun and Terry Barnett

Hoop Tensile Properties of Ceramic Matrix Composite Cylinders

ABSTRACT: Tensile stress-strain properties in the hoop direction were obtained for 100-mm diameter SiC/SiC ceramic matrix composite cylinders using ring specimens machined from the cylinder ends. The cylinders were fabricated from 2D balanced SiC fabric with several material variants, including wall thickness (6, 8, and 12 plies), SiC fiber type (Sylramic, Sylramic-iBN, Hi-Nicalon, and Hi-Nicalon S), fiber sizing type, and matrix type (full CVI SiC, and partial CVI SiC plus slurry cast + melt-infiltrated SiC-Si). Fiber ply splices existed in all the hoops. Tensile hoop measurements were made at room temperature and 1200°C using hydrostatic ring test facilities. The failure mode of the hoops, determined through microstructural examination, is presented. The hoop properties are compared with in-plane data measured on flat panels using same material variants, but containing no splices.

KEYWORDS: ceramic matrix composite, silicon carbide fibers, composite structures, mechanical properties

Introduction

Silicon carbide fiber-reinforced silicon carbide (SiC/SiC) ceramic matrix composites are being evaluated for use as a combustor liner material for gas turbine engines [1-6]. Many ceramic matrix composite (CMC) full annular combustor designs are under evaluation [4-6], but these designs are often structurally analyzed using data generated from specimens machined from flat panels. Typical annular combustor liner operation requires the SiC/SiC material to resist thermal gradients that produce tensile and compressive stresses in the circumferential (hoop) direction and bending stresses in the axial direction [7]. Also, the structural properties of CMC parts can sometimes be significantly different than those of panels because of changes in fiber architecture required to make shapes and because of difficulties in replicating panel processing conditions [8]. To assess whether property issues could exist even for simple combustor designs, tensile stress-strain curves were measured in the hoop direction for SiC/SiC cylinders with several material variants, including wall thickness, fiber type, and matrix type. The purpose of this paper is to report the hoop tensile properties and failure modes of these different SiC/SiC materials and to compare these properties to those obtained from flat panels fabricated with the same constituents.

Experimental

Materials and Specimens

Eight 250-mm long SiC/SiC cylinders were fabricated from 2D-balanced 5-harness satin [0/90] fabric by GE Power Systems Composites. Material variations of the 100-mm diameter cylinders included wall thickness (6, 8, and 12 plies), SiC fiber type (Sylramic, Sylramic-iBN,

Hi-Nicalon, and Hi-Nicalon type S), fiber sizing type (1 and 2), and matrix type (full CVI SiC, and partial CVI SiC plus slurry cast + melt-infiltrated (MI) SiC-Si). Use of sizing 2 in Sylramic-reinforced MI SiC composites results in improved high temperature panel properties when compared to the same composite fabricated with sizing 1 [8]. All cylinders had a volume fraction of 35 +/- 3% of BN-coated fibers, which were aligned along the axial and hoop [0/90] directions. One butt splice running along the axial direction was used to join each fabric ply around the cylinder circumference. For example, an eight-ply cylinder had eight-ply splices 45° apart (Figure 1). To minimize structural interactions, splices in adjacent plies were separated by 135° in the circumferential direction. Table 1 lists key constituents for each cylinder.

A ring specimen of 10.1 mm in height was machined from each end of each cylinder. One specimen from each cylinder was tested at room temperature and one specimen from seven of the eight cylinder types was tested at 1200 °C.

TABLE 1 – SiC/SiC material constituents for cylinders tested.

ID	Fiber Type	Fiber v/o	EPI[a]	Plies[b]	Matrix Type
021	Hi-Nicalon	33.8	17	8	(CVI + MI) SiC-Si
003	Hi-Nicalon type S	33.4	18	8	(CVI + MI) SiC-Si
005	Sylramic with sizing 1	38	20	8	(CVI + MI) SiC-Si
007	Sylramic with sizing 2	38	20	8	(CVI + MI) SiC-Si
013	Sylramic-iBN	35.6	20	6	(CVI + MI) SiC-Si
015	Sylramic-iBN	37.2	20	12	(CVI + MI) SiC-Si
009	Sylramic with sizing 2	38	20	8	(full CVI) SiC
017	Sylramic-iBN	32.8	20	8	(full CVI) SiC

[a] EPI = tow ends per inch

[b] wall thickness ~ 0.25 mm per ply

Test Procedures

Hoop tensile properties were obtained using hydrostatic ring test facilities [7]. The ambient temperature facility applies pressure to the inner diameter of the rings using hydraulic oil in a rubber bladder (see Figure 2). The rubber bladder mates to the inner diameter of the ring specimens, causing expansion of the specimens. A pressure transducer measures the hydraulic oil pressure applied to the rings via the bladder. The tensile hoop stress (σ) can be calculated using mechanics of materials relationship for a thin walled pressure vessel subjected to a uniform internal pressure:

$$\sigma = pr_i/t \qquad (1)$$

where p = internal pressure, r_i = inner radius of the ring, and t = wall thickness. The average stress through the thickness of the cylinder wall is calculated using Equation 1. A string was wrapped around the outside of the hoops and attached to two string-loaded linear variable differential transformers (LVDTs) in order to measure outer-diameter circumferential strain with applied pressure. Two strain gages, applied 180° apart on the outside of the rings, were also used to measure strain. The data obtained with this facility include ultimate hoop tensile strength, hoop elastic modulus, and hoop tensile failure strain.

A similar procedure was used to obtain hoop tensile properties at 1200 °C [7]. The elevated temperature facility includes 18 cooled wedges that mate with the inner diameter of the hoop specimens (Figure 3). Hydraulic pressure is applied through a rubber bladder, which mates with the inner diameter of the wedges. The cooled wedge configuration is required to maintain the bladder near room temperature while heating the specimens to elevated temperatures using a resistively heated furnace. Strain was measured using LVDTs in a similar fashion as used for room temperature testing. Stress was calculated at 1200 °C using the same formula used at room temperature (Eq. 1). The applicability of this relationship to calculate stress in the elevated temperature facility was verified at room temperature using instrumented aluminum and steel calibration rings [9].

In-plane tensile properties were also obtained using 25-mm gauge length dog-boned specimens from SiC/SiC panels manufactured by GE Power Systems Composites with the same constituents and fabric architectures used to make some of the cylinders, but without the presence of ply splices. The test procedures followed those recommended by ASTM [10].

Results

Mechanical Properties

Hoop tensile properties from single specimens of each of the different materials were obtained. To estimate property standard deviations, data that exists for SiC/SiC combustor cans can be used. The combustor cans were fabricated for combustion testing in the Rich-Burn, Quick Quench, Lean-Burn (RQL) sector rig [11]. Over twenty-five Rich Zone Liner (RZL) combustor cans were manufactured using the same constituents in cylinder 005 (Table 1). Two 125 mm diameter hoop tensile specimens were machined from excess material of the RZLs and were tested using the ambient temperature hydrostatic ring test facility to obtain as-fabricated material properties. Table 2 summarizes the average hoop tensile properties and standard deviations obtained from one lot of twelve RZLs. The data obtained for the cylinders tested in this study can be examined if it is assumed that they have similar standard deviations at 23 and 1200 °C as the RZL hoops.

Table 2 – Room temperature hoop strength properties obtained through testing of witness coupons machined from SiC/SiC Rich Zone Liner combustor cans.

	Strength, MPa	Modulus, GPa	Strain to Failure, %
Average of 24 tests	142	277	0.052
Standard deviation	15.2	16.3	0.008

Figure 4 shows that the room temperature hoop strengths for the eight cylinders were generally similar (about 200-220 MPa). Exceptions existed for the one cylinder with Hi Nicalon type S (003) and the one cylinder with Sylramic fibers in CVI full SiC matrix (009), which had lower strengths. Hoop failure strains generally correlated with the strength values. Exceptions were the cylinder reinforced by the Hi-Nicalon fibers (021), which displayed strains higher than predicted based on linear-elastic behavior, and the cylinder reinforced by Hi-Nicalon S (003) and cylinder 017 (Sylramic-iBN/CVI SiC matrix), which had lower failure strains.

For the hoop tensile properties obtained at 1200°C, Figure 5 shows that in essentially all cases, ultimate strengths and strains were about 70% of their room temperature values, and elastic moduli were slightly changed at about 90-100% of their room temperature values. An exception was the Sylramic fiber reinforced MI cylinder (007), which retained 50% of the strength relative to the room temperature panel strength and also had the highest modulus.

The room temperature and 1200°C stress-strain curves for several cylinders are compared to that for panels fabricated from the same constituents in Figure 6. Data for the different materials are offset along the strain axis. Both the hoop and panel specimen have the same initial tensile behavior. At room temperature, the hoops failed at a stress that was about 50% of the panel strength. The 1200 °C hoop strength was about 40% of panel strength. Because of the slight deviation from linear-elastic behavior, cylinder ultimate strain was considerably less then that for panels (about 25 and 17% of panel failure strain at room temperature and 1200 °C, respectively). The exception was the Hi-Nicalon reinforced MI SiC matrix cylinder (021), which had significant non-linear strain response and had almost 90% of the room temperature panel strength.

Examination of Tested Specimens

Failed hoops were examined to determine failure modes. Most of the specimens fractured into two or more pieces, especially those tested at room temperature. The exceptions were the MI SiC matrix cylinders reinforced with Hi-Nicalon (021) and Hi-Nicalon S fibers (003), which fractured at only one location after room temperature and 1200 °C testing.

Examples of fractured hoops are shown in Figure 7. In Figure 7a, the cylinder specimen that had the most damage can be seen. A 12-ply Sylramic-iBN /MI SiC matrix hoop (015) broke into 9 pieces after room temperature testing. Another hoop cut from this same cylinder broke into only 3 pieces after 1200 °C testing and had similar strength and modulus as the hoop broken into 9 pieces. The hoop that had the highest room temperature strength, the Sylramic-iBN/CVI SiC matrix specimen (017), broke into two pieces (Fig. 7a).

In general, hoops tested at 1200 °C fractured into fewer pieces. A cylinder with Sylramic fibers/MI SiC matrix (007) had the most damage (Fig. 7b), breaking into three pieces. The hoop specimen with Hi-Nicalon S fibers/ MI SiC matrix (003) fractured at one location (Fig. 7b).

Boroscope examination between combustion rig testing runs of SiC/SiC RZL combustor cans with the same fiber architecture as these cylinders revealed that cracking initiated on fiber cloth ply splices [11]. Based on this data, fracture of the hoop specimens would be expected at fiber ply splices. The locations of the ply splices used to fabricate each cylinder tested in this study were documented by the composite manufacturer (see Figure 1 for schematic of eight ply hoops). Microstructural sections taken from the failed specimens were examined to find ply splices. By locating a particular ply splice, one could locate fracture surfaces relative to the positions of all the ply splices.

As an example of the procedure used to find the location of fracture surfaces relative to the fiber cloth splices is as follows. After being tested at room temperature, hoop 013 fractured into four pieces, two covering a 60° arc and two covering a 120 °arc. The ply splices in a six ply hoop, such as specimen 013, are separated by 60°. Figure 8 shows the cloth lay up for the six ply hoops. A section was cut from the middle of one of the 120 ° arc sections to look for a ply splice. This cross-section from hoop 013 was mounted in epoxy and polished. The microstructure is shown in Figure 9. A splice can be seen in a ply near the outer diameter, in the fifth of the six plies (the sixth ply is on the outer diameter). Knowing the exact location of this splice in the fractured rig section, one can determine of location of the fracture surfaces by

orienting the ply splice 5 and the fractured sections with the cloth lay up diagram as shown in Figure 8. The results of this procedure revealed that hoop 013 fractured at ply splices 1 (the inner diameter splice) 2, 3, and 6 (the outer diameter splice). This procedure was conducted for eight of the sixteen hoop specimens tested. A summary of these results is given in Table 3. Note that every hoop specimen examined had a fracture surface at ply splice 1, the inner most ply.

Table 3 – Fracture Locations for SiC/SiC Tested Under Hoop Tensile Loading

Hoop ID	Test Temperature, °C	Fracture Surface Location
005	23	Ply splices 1 and 2
007	23	Ply splices 1 and 5
013	23	Ply splices 1, 2, 3, and 6
009	23	Ply splices 1, 7, and 8
017	23	Ply splice 1
003	1200	Ply splice 1
007	1200	Ply splices 1 and 5, and between ply splices 2 and 6
013	1200	Ply splices 1 and 5

Discussion

From Figure 6, it can be concluded that the hoops had the same modulus and initial stress-strain behavior as standard tensile measurements on flat panel specimens with the same constituents and fiber architectures but no ply splices. The major differences were the reduced ultimate stress and strain values of the hoops, which can be attributed to local fiber architectural differences caused by the presence of butt ply splices in the hoops. Discontinuous fiber cloth and matrix-rich regions exist in the splices. However, ply splices are necessary when 2D fabric is used to make complex composite parts, such as full annular combustor liners.

One simple explanation for the lower ultimate strength and strain for the cylinders is that at each butt splice, the local fiber volume fraction in the hoop or stress direction was reduced to a factor (N-1)/N times the global fiber fraction, where N is the number of plies. For 8-ply cylinder having a nominal 35 v/o of fibers, the local fiber volume fraction at a splice would be about 30 %. Ignoring any stress concentration effects, one would expect strength should slightly less (based on a rule of mixtures analysis) than the flat panel strength. However, for composites with the same 2D fabric, ring tensile strength is typically 40 to 50% of panel specimens (see Figures 4 and 5). This suggests that local stress concentrations existed around the butt splices because of the fiber discontinuity. Since the ultimate strains for the hoops were typically above those required for matrix cracking, it would appear that these stress concentrations probably caused local fiber fracture in neighboring plies, with ultimate specimen fracture likely occurring at one of the 8 butt splices around the 8 ply ring specimens.

As seen in examination of tested hoops (summarized in Table 3), a primary location for ring fracture was at the butt splice for the inner cylinder ply. A potential reason for this predominant failure location is higher local stresses at the inner diameter. The stress calculated using Equation 1 is the average stress through the thickness of the hoop. This equation is applicable for

cylinders that have a wall thickness/inner diameter < 1/20, such as the 6 and 8 ply hoops. To calculate the radial stress distribution in a cylinder subjected to uniform internal pressure, such as these hoops tested using the hydrostatic facility, the relationship for a thick walled cylinder can be used. The tensile hoop stress (σ) for a thick walled cylinder is [16]:

$$\sigma = [pr_i/(r_o^2 - r_i^2)] * [1-(r_o/r)^2] \quad (2).$$

The internal pressure is p, the inside radius of a ring is r_i, the outside radius is r_o, and r is the radial location at any point between r_i and r_o. At the inner surface of a hoop, ($r = r_i$), the stress is maximum and at the outside of a hoop ($r = r_o$), the stress is minimum. For a six ply hoop (013), the stress at the ID is 1.5% greater than the average stress and the stress at the OD is 1.5% less. Calculations for eight ply hoops (005 and 007) revealed that the stress at the ID is 2.3% greater than the average stress calculated using Eq. 1, while the stress at the ID for the twelve ply hoops is 3.4% greater. Thus, for all hoop types, the peak stress at the ID is only slightly greater than the average stress. This suggests that stress concentration associated with the splice geometry is responsible for fracture at the inside ply splice and that the peak stress that the inner diameter has little effect on the hoop fracture process. Recent tensile data generated on iBN-Sylramic MI panel specimens with splices (the same material constituents in hoops 013 and 015) revealed that the presence of a ply splice on the composite surface reduced strength, but ply splices in the interior plies had little effect the tensile behavior [12]. This data confirms the deleterious effect of ply splices on the strength of hoops relative to that for flat panels without splices.

The Hi-Nicalon hoops had high strengths and failure strains two times greater than any of the other hoop materials, both at room temperature and 1200 °C. One possible reason for these good properties may be that the Hi-Nicalon cylinder was the highest quality of all those produced. However, microstructural examination results of the Hi-Nicalon hoop tested at room temperature was inconclusive. A more probable explanation may be that since Hi-Nicalon MI composites in panel form typically have higher tensile failure strain than iBN-Sylramic or Sylramic MI composites [13, 14], this trend may exist in the cylinders having the same constituents. Also, from Figure 6, it appears that the Hi-Nicalon cylinder is less susceptible to the stress concentrations associated with the presence of the ply splices than the other hoops, since the strength of the Hi-Nicalon hoop is about only 11% less than the strength of a specimen machined from a Hi-Nicalon panel (with continuous cloth). One could conclude from this behavior that the slight strength debit of this hoop is due to the smaller local fiber volume fraction at the ply splices. It is important to note that iBN-Sylramic or Sylramic MI composites in panel form have better high temperature strength and durability than Hi-Nicalon MI composites [13].

The hoop tensile test was used to compare properties of SiC/SiC cylinders with various constituents. CMC components proposed for turbine engine applications, such as combustor liners, turbine vanes, and exhaust nozzle flaps and seals, will be required to operate at high temperatures for up to thousands of hours. Durability testing of hoops would be a better discriminator for the different materials for engine applications and would better approximate properties of an annular part rather than data from flat panels. For example, a cylinder tested in this study containing a CVI SiC matrix (017) had good strength and modulus at both 23 and 1200 °C. In contrast, a CVI SiC matrix, Nicalon fiber combustor liner that was field tested in a turbine engine for 5000 hours had more damage than a liner having an MI SiC matrix reinforced

by Hi Nicalon fibers [15]. The better performance of the Hi Nicalon/MI SiC matrix liner was attributed to its higher conductivity and density.

Summary and Conclusions

The hoop tensile stress-strain properties were measured at room temperature and 1200°C for eight SiC/SiC cylinders reinforced with 2D fiber cloth and fabricated from a variety of constituents. For each temperature, ultimate strength, strain, and elastic modulus were generally similar for the cylinders, but strength and strain values were a significantly lower fraction, about 40 to 50% and about 20%, respectively, of those measured for flat SiC/SiC panels fabricated with the same 2D fabric and constituents. Ultimate strength and strain debits were caused by the presence of butt ply splices, which were needed to join plies along the axial direction of the cylinders. The large amount of knockdown is attributed to reduced fiber content at the butt splices and to further fiber loss during matrix cracking at the splices. Examination of the tested hoops revealed that fracture occurred at the locations of butt ply splices. A fracture surface always existed at the splice on the inner diameter of the failed specimens.

References

1. Brewer, D., Ojard, G., and Gibler, M., "Ceramic Matrix Composite Combustor Liner Rig Test", ASME paper TE00CER03-03, May, 2000.
2. Ojard, G., Stephan, R., Naik, R., Gibler, M., Cairo, R., Linsey, G., Hornick, J., and Brewer, D., "NASA Rich Burn Quick Quench Lean Burn Sector Rig SiC/SiC CMC Testing", in proceedings of 24th Annual Conference on Composites, Materials, and Structures, Cocoa Beach, FL., Jan., 2000.
3. Corman, G., Dean, A., et. al, "Rig and Gas Turbine Testing of MI-CMC Combustor and Shroud Components", ASME paper 2001-GT-0593, 2001.
4. Shi, J.,"Design, Analysis, Fabrication and Testing of a CMC Combustion Can", ASME paper 2000-GT-71, 2000.
5. Miriyala, N., Kimmel, J., Price, J., More, K., Tortorelli, P., Eaton, H., Linsey, G., and Sun, E., "The Evaluation of CFCC Liners after Field Testing in a Gas Turbine – III", ASME paper GT-2002-30585, 2002.
6. Igashira, K.-I., Matsubara, G., Matsuda, Y., and Imamura, A., "Development of the Advanced Combustor Liner Composed of CMC/GMC Hybrid Composite Material", ASME paper 2001-GT-0511.
7. Barnett, T. R., Ojard, G. C., and Cairo, R. R., "Relationships of Test Methods and Standards Development to Emerging Retrofit CFCC Markets", in ASTM STP 1392, M. G. Jenkins, E. Lara-Curzio, and S. T. Gonczy, Eds., American Society for Testing and Materials, West Conshohoken, PA, 2000.
8. DiCarlo, J.A., and Yun, H.M., NASA Glenn Research Center, unpublished research.
9. Starrett, S., Johnsen, B., and Gillis, P., "Analytical Study of the High Temperature Tensile and Compressive Ring Tests", proceedings of JANNEF meeting held in Monterey, CA, 1982.
10. ASTM Standard C 1359-96, "Standard Test Method for Monotonic Tensile Strength Testing of Continuous Fiber-Reinforced Advanced Ceramics with Solid Rectangular Cross-Section Specimens at Elevated Temperatures", Annual Book of ASTM Standards, vol. 15.01, 2000.

11. Verrilli, M. J., Martin, L. C., and Brewer, D. N., "RQL Sector Rig Testing of SiC/SiC Combustor Liners", NASA TM 2002-211509, April 2002.
12. Calomino, A. and Verrilli, M. J., "Mechanical Performance Improvements of an In-situ Boron Nitride-coated MI SiC/SiC Composite", in the proceedings of the 26th Annual Conference on Composites, Materials, and Structures, held in Cocoa Beach, FL, Jan. 28-31, 2002.
13. Yun, H.M., DiCarlo, J.A., and Bhatt, R.T., "Processing and Structural Advantages of the Sylramic-iBN SiC Fiber for SiC/SiC Components", Ceramic Engineering and Science Proceedings, vol. 24, [4,], pp. 247-253, 2003.
14. Yun, H.M. and DiCarlo, J.A., "Effects of 2-D Fabric Geometry on the Tensile Strength of Stoichiometric SiC Fiber-Reinforced Composites", in *High Temperature Ceramic Matrix Composites*, W. Krenkel, R. Naslain, and H. Schneider, Eds, Wiley-VCH, Weinheim, Germany, 2001, pp. 99-105.
15. Miriyala, N. and Price, J., "The Evaluation of CFCC Liners after Field Testing in a Gas Turbine – II", ASME paper 2000-GT-648, 2000.
16. Popov, E.P., Mechanics of Materials, 2rd Edition, Prentice-Hall, Englewood Cliffs, New Jersey, 1976.

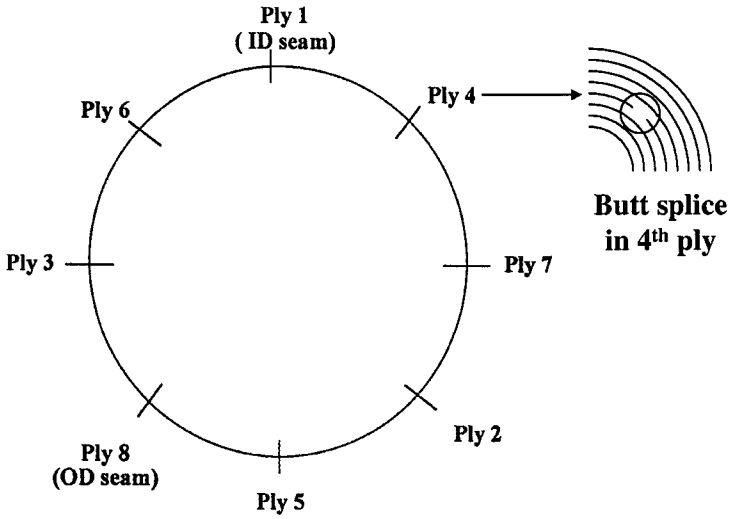

Figure 1 – Schematic of the cylinder cross section showing locations of the ply splices used to fabricate an eight ply, 100 mm outer diameter cylinder using 0/90 5HS SiC cloth.

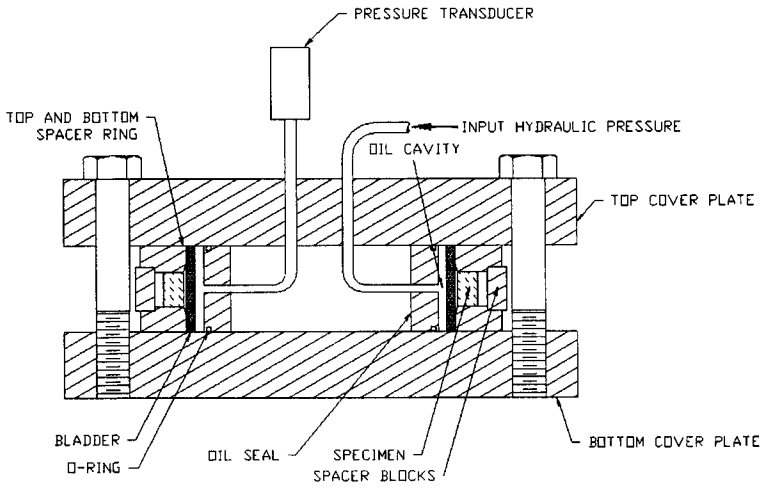

Figure 2 – Schematic of the room temperature hydrostatic test facility.

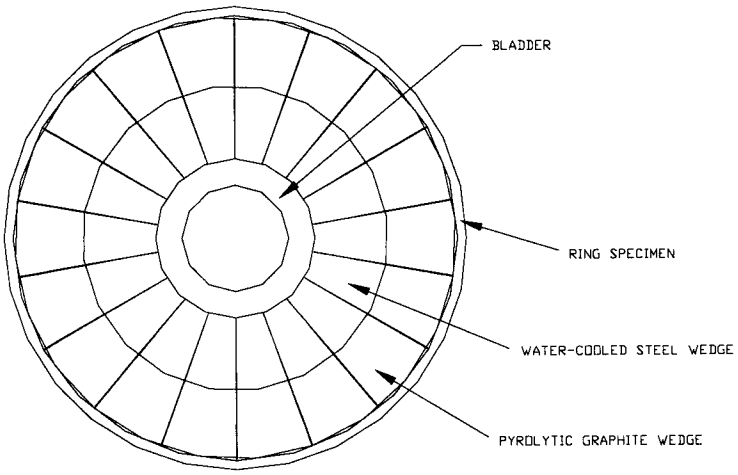

Figure 3 – Schematic of the elevated temperature hydrostatic test facility showing the wedge assembly.

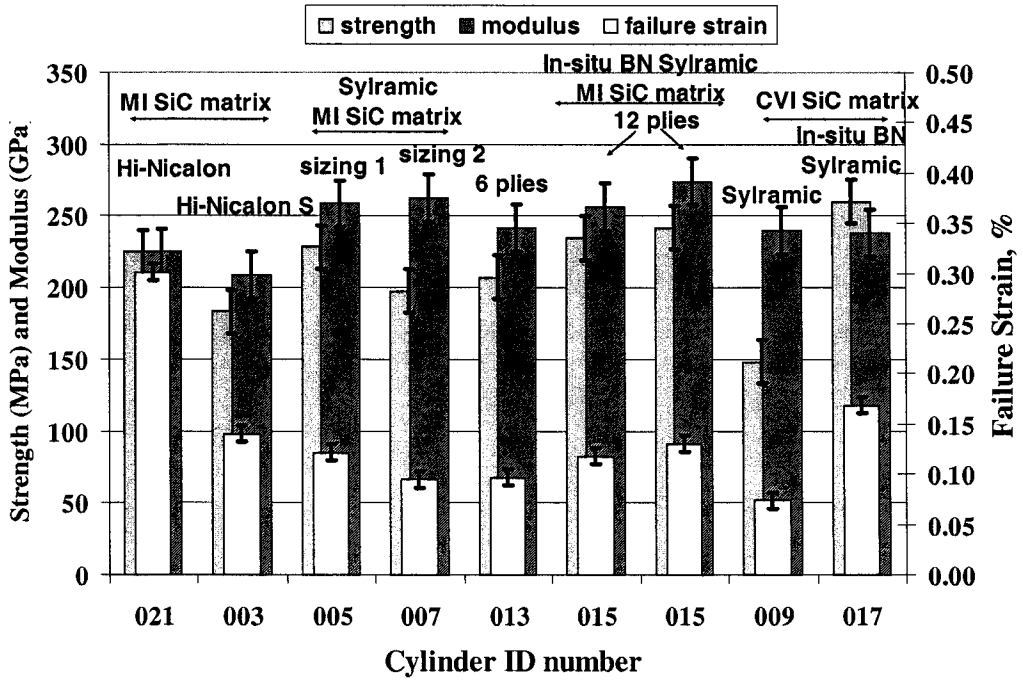

Figure 4 – Ultimate strength, strain, and modulus for SiC/SiC cylinders measured at room temperature.

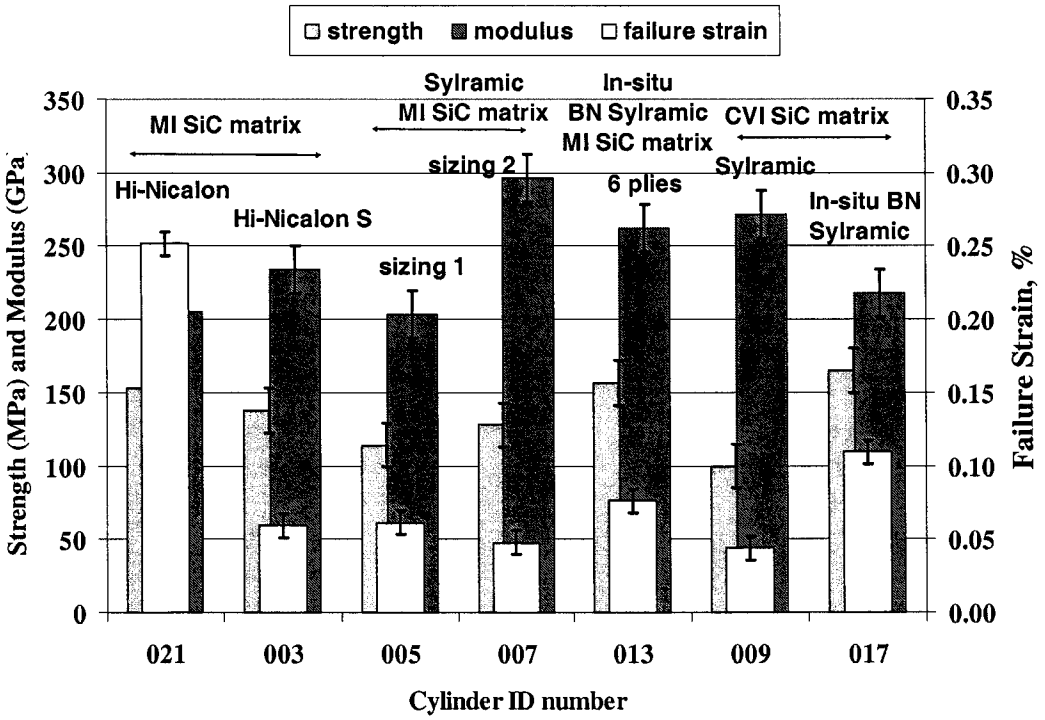

(b)

Figure 5 – Ultimate strength, strain, and modulus for SiC/SiC cylinders measured at 1200 °C.

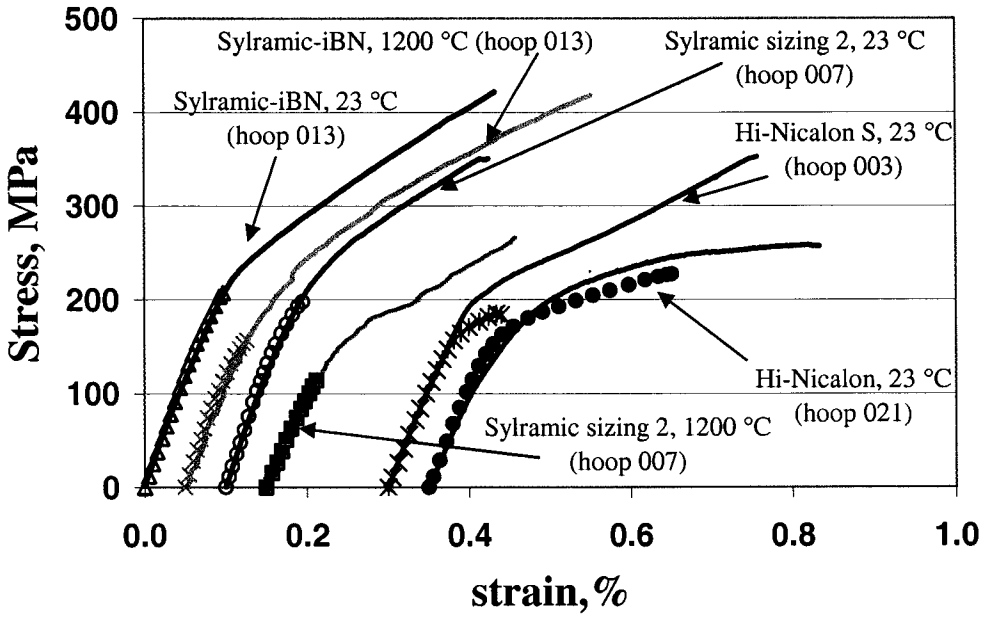

Figure 6 – Room temperature and 1200 °C stress-strain behavior for SiC/SiC hoops and panels fabricated using the same constituents. All specimens tested had a CVI +MI matrix. The lines are the panel data and the symbols are data for the hoops. Data for the different materials are offset along the strain axis.

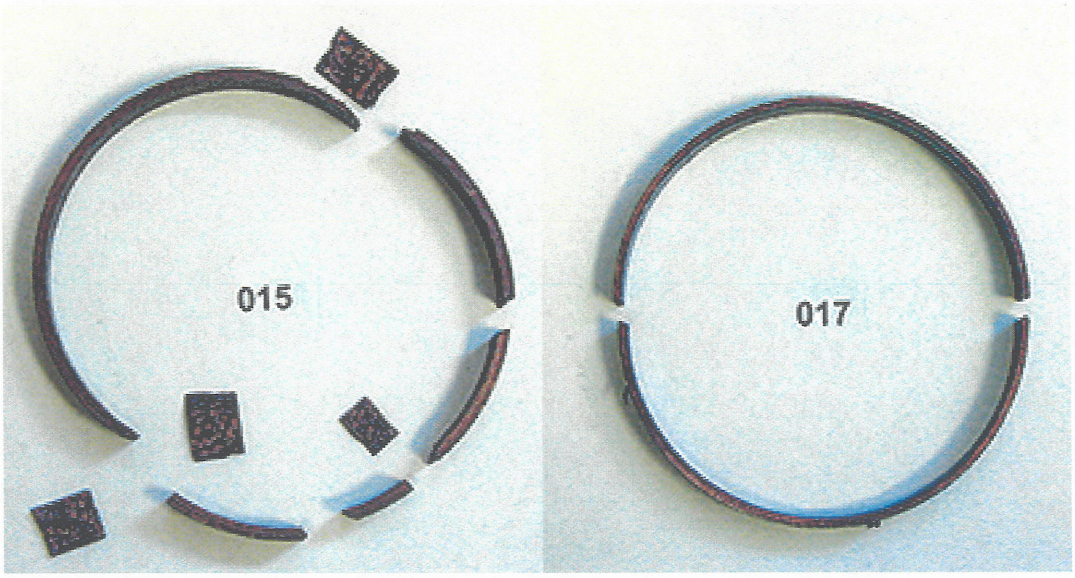

a.

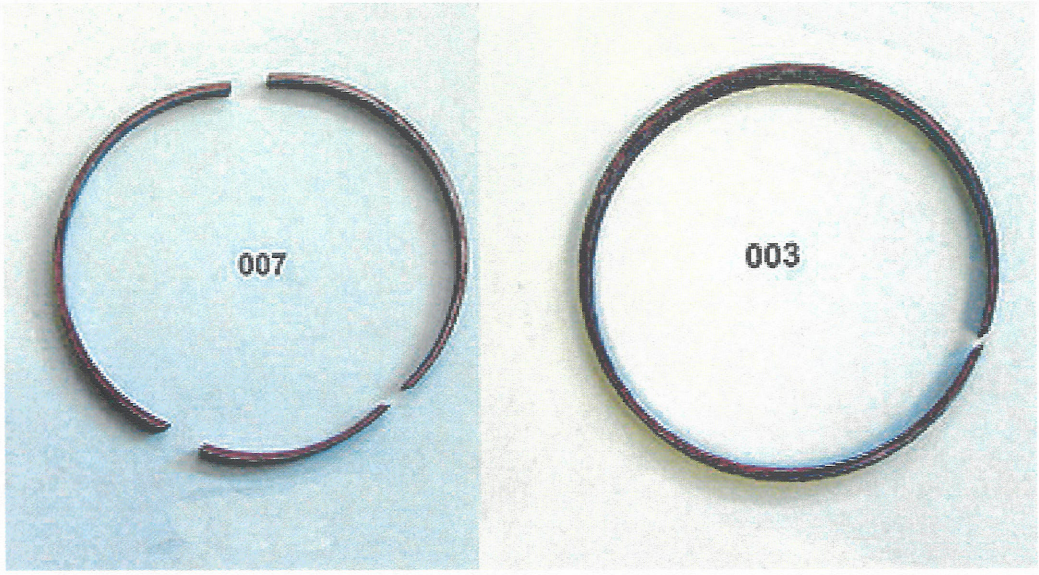

b.

Figure 7 – Examples of SiC/SiC cylinder specimens after hoop tensile testing, a) at room temperature, b) at 1200 °C.

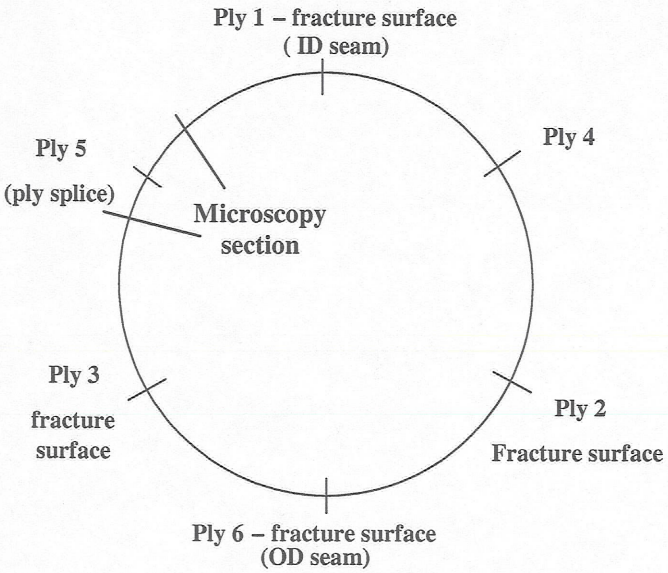

Figure 8 – Schematic of ply lay up for 6 ply SiC/SiC cylinders. The fracture locations and location of a microscopy section for hoop 013, which was tested at room temperature, are shown as well.

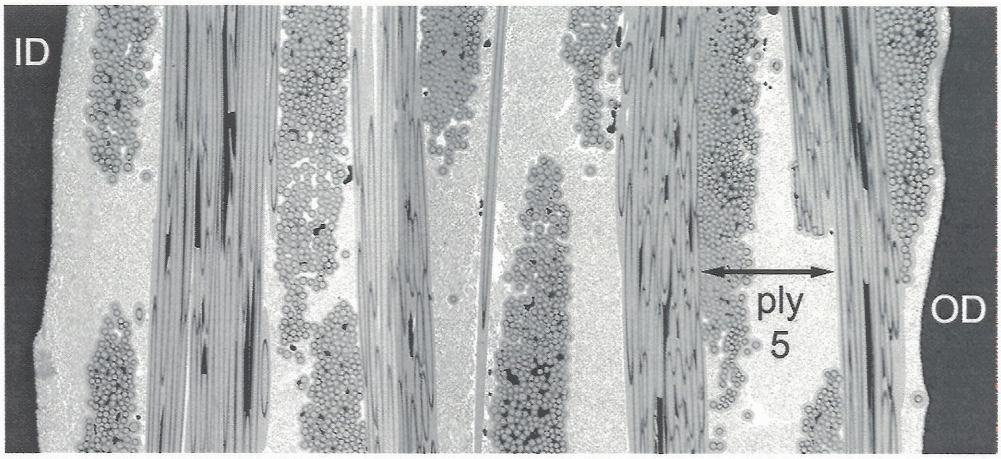

Figure 9 – Cross-section of hoop 013 tested at room temperature. The ply splice can be seen in 5th ply of this 6 ply composite